

# Modeling sound attenuation in heterogeneous environments for improved bioacoustic sampling of wildlife populations

**J. Andrew Royle**

USGS Patuxent Wildlife Research Center

Laurel, MD 20708

email: aroyle at usgs.gov

January 13, 2018

1 **Abstract** Acoustic sampling methods are becoming increasingly important in biological  
2 monitoring. Sound attenuation is one of the most important dynamics affecting the utility  
3 of bioacoustic data as it directly affects the probability of detection of individuals from  
4 bioacoustic arrays and especially the localization of acoustic signals necessary in telemetry  
5 studies. Therefore, models of sound attenuation are necessary to make efficient use of  
6 bioacoustic data in ecological monitoring and assessment applications. Models of  
7 attenuation in widespread use are based on Euclidean distance between source and sensor,  
8 which is justified under spherical attenuation of sound waves in homogeneous  
9 environments. In some applications there are efforts to evaluate the detection range of  
10 sensors in response to local environmental characteristics at the sensor or at sentinel source  
11 locations with known environmental characteristics. However, attenuation is a function of  
12 the total environment between source and sensor, not just their locations. In this paper I  
13 develop a model of signal attenuation based on a non-Euclidean cost-weighted distance  
14 metric which contains resistance parameters that relate to environmental heterogeneity in  
15 the vicinity of an array. Importantly, these parameters can be estimated by maximum  
16 likelihood using experimental data from an array of fixed sources, thus allowing

17 investigators who use bioacoustic methods to devise explicit models of sound attenuation  
18 *in situ*. In addition, drawing on analogy with classes of models known as spatial  
19 capture-recapture, I show that parameters of the non-Euclidean model of attenuation can  
20 be estimated when source locations are *unknown*. Thus, the models can be applied to real  
21 field studies which require localization of signals in heterogeneous environments.

22 **Key words:** acoustic monitoring, bioacoustics, distance sampling, sound attenuation,  
23 spatial capture-recapture, telemetry, least-cost path models

24 **Running title.** Modeling sound attenuation

## 25 **1 Introduction**

26 Acoustic sampling technology has emerged as an important method for the study of vocal  
27 species such as birds, anurans, marine mammals, many species of fish, and primates, or  
28 for species to which acoustic transponders can be implanted or affixed to. As a result,  
29 the deployment of automated acoustic recording devices has proliferated rapidly in both  
30 terrestrial (Blumstein et al. 2011; Digby et al. 2016; Brauer et al. 2016; Measey et al. 2017)  
31 and aquatic (Marques et al. 2009; Kessel et al. 2013; Marques et al. 2013; Cooke et al.  
32 2016; Crossin et al. 2017) systems.

33 Bioacoustic technology is broadly relevant to the study of spatial ecology of animal popu-  
34 lations. Two specific uses which are the focus of this paper are the application of bioacoustics  
35 to density estimation using variations of spatial capture-recapture (SCR) methods (Efford  
36 et al. 2009; Marques et al. 2013; Stevenson et al. 2015; Kidney et al. 2016) and its use  
37 in acoustic telemetry (Heupel et al. 2006) for the study of movement and resource selec-  
38 tion. Acoustic telemetry has become widely used in aquatic environments to study fish, sea  
39 turtles, and marine mammals. Use of acoustic data for either SCR or telemetry requires  
40 *localization* of the observed signals obtained from acoustic data. This is essentially statisti-

cal triangulation which can be done when signals are obtained from an array of bioacoustic sensors so that potentially multiple detections of the same signal are possible (Janik et al. 2000; McGregor et al. 1997; Bower and Clark 2005; Blumstein et al. 2011). The precision of source localization improves with the number of sensors in the array and the density of the array. Localization has been recognized as being analogous to inference about the activity center in SCR methods, and therefore SCR has been adapted to accommodate data obtained by acoustic sampling methods (Dawson and Efford 2009; Efford et al. 2009; Borchers et al. 2015; Stevenson et al. 2015; Kidney et al. 2016).

Localization of acoustic sources requires explicit models for sound attenuation, i.e., the energy loss of sound propagation through a medium. In general, attenuation depends on the properties of the medium (Wiley and Richards 1982), and this often is characterized experimentally by engineers to satisfy design objectives of acoustic systems. However, to date, applications of bioacoustic methods in ecology have used simplistic models of spherical attenuation, in which amplitude decays according to a power law with rate proportional to the inverse of Euclidean distance<sup>1</sup>. In practice, sound attenuation is strongly affected by the structure of the environment between the source origin and the receiver (Singh et al. 2009; Kessel et al. 2013; Rek and Kwiatkowska 2016; Selby et al. 2016). When the environment is highly heterogeneous Euclidean distance models may be inadequate. For example in bird monitoring problems there may be substantial variability in vegetation density or height in the vicinity of a sensor or array of sensors. In acoustic telemetry studies, the attenuation of the signal can depend on depth, substrate, surface conditions and many other factors (Selby et al. 2016). This has led to considerable recent attention to the problem of “range testing” to determine effective detection range given environmental heterogeneity for acoustic telemetry applications (Marques et al. 2009; Kessel et al. 2013; Selby et al. 2016). For example, Selby et al. (2016) model attenuation as a function of source and sensor specific covariates (e.g., depth). However, attenuation of signals depends on the total environment between the

---

<sup>1</sup>e.g., see [https://en.wikipedia.org/wiki/Acoustic\\_attenuation](https://en.wikipedia.org/wiki/Acoustic_attenuation) accessed 12/20/2016.

67 signal and the source and therefore more general models of attenuation are needed.

68 Ideally, the end use of bioacoustic data in monitoring and assessment of biological pop-  
69 ulations should integrate explicit models of sound attenuation with parameters that are  
70 themselves estimated *in situ* along with biological parameters of interest such as density,  
71 position of sources, occupancy, or other ecological state variables. In this paper I sug-  
72 gest flexible classes of models for modeling attenuation in heterogeneous environments using  
73 cost-weighted distance in which effective distance is defined by a cost function that involves  
74 spatially explicit structure describing a heterogeneous landscape. This non-Euclidean dis-  
75 tance model is widely used in least-cost path model analysis (Adriaensen et al. 2003) of  
76 landscape connectivity. Inference under this model has been formalized in the context of  
77 spatial capture-recapture studies (Royle et al. 2013; Sutherland et al. 2015; Fuller et al.  
78 2016) as a model to describe movements of individuals about their home range, and also as  
79 a model for dispersal of individuals (Graves et al. 2014).

## 80 **2 Data structure and model**

81 Consider an idealized acoustic sampling array shown in Figure 1, which suppose is a 600 m  
82 x 600 m block of forest for which lidar measurements are available and aggregated to 20  $m^2$   
83 resolution showing a standardized form of average vertical vegetation density at each point  
84 (color-coded in Fig. 1). Within this landscape an array of 9 bioacoustic sensors is situated  
85 in a regular grid, and among the sensor array are located 16 experimental sources producing  
86 vocalizations that may or may not be detected at each sensor. In practice one might imagine  
87 more attenuation between a source and sensor when dense habitat (green) predominates and  
88 less attenuation in open habitats such as gaps in the forest canopy (white).

The data from a field experiment of this sort are power or signal strength measurements,  $S_{ij}$ , at each sensor having location  $\mathbf{x}_j$ , from each source  $i = 1, 2, \dots, n$  ( $n = 16$  in this case) having location  $\mathbf{s}_i$ . The model for these observations can be formulated in terms of other

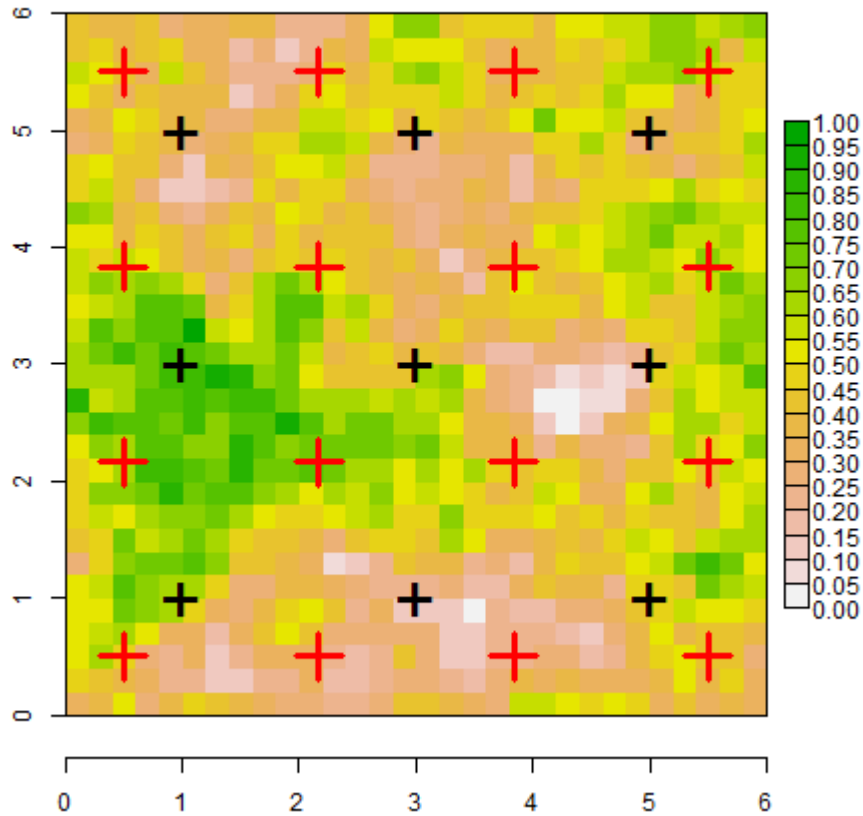


Figure 1: Idealized system showing an array of 9 sensors and an array of 16 experimental sources (e.g., speakers producing vocalizations of a species). Habitat structure is illustrated here as a standardize variable of vegetation density with high vertical density (green) representing dense vegetation and low vertical density (white) representing open areas.

signal characteristics such as time of arrival (Stevenson et al. 2015) but here for clarity I adhere to a formulation in terms of signal strength alone, although the basic ideas are the same. Following Efford et al. (2009) assume a transformation of signal strength that declines with distance  $d$  from the source, and assume the transformation produces a normally distributed variable such that attenuation is well approximated by the model

$$S_{ij} = \alpha_0 + \alpha_1 d(\mathbf{x}_j, \mathbf{s}_i) + \epsilon_{ij} \quad (1)$$

89 where  $\epsilon_{ij} \sim \text{Normal}(0, \sigma^2)$  is noise. When the signal strength takes on positive values then the  
90 log-transformation would normally be satisfactory, and furthermore this is the natural scale  
91 when power is measured in decibels (dB). Sounds are detected when  $S$  exceeds a threshold  
92  $c$  (Dawson and Efford 2009) which is somewhat arbitrary but should be set above the mean  
93 level of ambient noise of the system so that detections are certain to be real. The signal  
94 to noise ratio can be directly characterized from observed data (Dawson and Efford 2009).  
95 For an experimental setting where the acoustic sources are known and only detection and  
96 signal strength at each receiver are random variables, the observed data are  $(y_{ij}, S_{ij})$  where  
97  $y_{ij} = 1$  if a signal from source  $i$  was detected at receiver  $j$  and  $y_{ij} = 0$  if the signal was not  
98 detected, and  $S_{ij} > c$  is the observed signal strength (transformed as noted above). Thus,  
99 the probability of detection is  $p_{ij} = \Pr(S_{ij} > c)$  which can be computed from the normal  
100 cumulative distribution function. When the observed signal strength is  $\leq c$  it is regarded as  
101 a missing value with probability  $1 - p_{ij}$ .

102 Equation 1 is a basic model of sound attenuation where the attenuation of sound in-  
103 tensity is governed by a single parameter  $\alpha_1$ , and relates only to the Euclidean distance  
104 between source and sensor,  $d(\mathbf{x}_j, \mathbf{s}_i)$ . Importantly, the form of this attenuation model is  
105 stationary (does not vary in space) and isotropic (it's two-dimensional contours are circular  
106 and symmetric). Intuitively, then, this model for signal strength is probably only suitable  
107 for homogeneous environments. In what follows I propose to generalize this model by allow-  
108 ing for the distance  $d(\mathbf{x}, \mathbf{s})$  to be both nonstationary and anisotropic using a non-Euclidean

109 distance metric that, in general, depends not only on the locations of sources and sensors  
110 but also on the composition of the landscape *between* them.

## 111 2.1 Cost-weighted distance models

An intuitively appealing model for sound attenuation in heterogeneous environments is the cost-weighted distance (CWD) model in which attenuation is governed not by Euclidean distance but by a cost-weighted distance metric which depends on the habitat structure in the vicinity of the sensor. The cost-weighted distance can be computed for a path  $\mathcal{P} = \{(v_1, v_2), (v_2, v_3), \dots, (v_m, v_{m+1})\}$  consisting of  $m$  segments between any two points  $\mathbf{v}_1$  and  $\mathbf{v}_{m+1}$  on the landscape and it is defined by

$$d_{cwd}(\mathbf{v}_1, \mathbf{v}_{m+1}) = \sum_g \text{cost}(\mathbf{v}_g, \mathbf{v}_{g+1}) * \text{dist}(\mathbf{v}_g, \mathbf{v}_{g+1}) \quad (2)$$

112 where  $\text{cost}(\mathbf{v}_g, \mathbf{v}_{g+1})$  is a parametric function describing the cost of movement between pixels  
113  $v_g$  and  $v_{g+1}$ , which must be prescribed (see below) and  $\text{dist}(\mathbf{v}_g, \mathbf{v}_{g+1})$  is the Euclidean distance  
114 between pixels. The cost-weighted distance then is the sum over all pixels along a given path  
115 connecting  $\mathbf{v}_1$  and  $\mathbf{v}_{m+1}$ . The least-cost path (LCP) (Adriaenson et al. 2003) is the path  
116 which has minimum CWD among all possible paths connecting the points  $\mathbf{v}_1$  and  $\mathbf{v}_{m+1}$ . In  
117 practice the cost-weighted distance between any two points and the least-cost path can be  
118 computed using the R package `gdistance` (van Etten 2017). Either the cost-weighted distance  
119 between points or the least-cost path can serve as an effective distance metric in models of  
120 sound attenuation, where parameter(s) of the cost function are estimated explicitly from  
121 data (see below).

The relevance of this distance metric to inference about sound attenuation arises when the cost function is parameterized in terms of the landscape structure. For example, if a covariate  $z(\mathbf{v})$  exists then one sensible function describing the cost of passing from pixel  $\mathbf{v}_g$

to pixel  $\mathbf{v}_{g+1}$  is

$$\text{cost}(\mathbf{v}_g, \mathbf{v}_{g+1}) = \frac{\exp(\alpha_2 z(\mathbf{v}_g)) + \exp(\alpha_2 z(\mathbf{v}_{g+1}))}{2} \quad (3)$$

The parameter  $\alpha_2$  represents the resistance of the covariate  $z(\mathbf{v})$  (higher values incur higher cost of transmission and *vice versa*), and it should be estimated from *observed* data on signal strength or time of arrival. I provide an estimation framework based on maximum likelihood below. To acknowledge this new distance metric in the model for sound attenuation, and that it depends on an unknown parameter  $\alpha_2$ , express the model as

$$S_{ij} = \alpha_0 + \alpha_1 d_{\text{cwd}}(\mathbf{x}_j, \mathbf{s}_i; \alpha_2) + \epsilon_{ij} \quad (4)$$

122 In general attenuation is frequency dependent (Wiley and Richards 1982) and thus param-  
123 eters  $\alpha_1$  and  $\alpha_2$  should depend on species.

124 Obviously any number of covariates can be included in the cost function Eq. 3. Note that  
125 if  $\alpha_2 = 0$  then the cost of transmission between any two pixels on the landscape is 1.0, and  
126 the cost-weighted distance reduces to Euclidean distance. As a practical matter we should  
127 scale any covariate  $z(\mathbf{v})$  to be in  $[0, 1]$  so that  $\alpha_2$  can be any real number. Negative numbers  
128 imply that increasing values of the covariate facilitate sound transmission and positive values  
129 imply that increasing values of the covariate impede sound transmission. The cost-weighted  
130 distance is conveniently computed in the R package `gdistance` using the `accCost` function, and  
131 the least-cost path between any two points can be computed using the function `costDistance`.

132 To see the effect of cost weighted distance on “effective distance” Fig. 2 shows contours  
133 of effective distance (in this case the least-cost path) for different values of the resistance  
134 parameter from Eq. 3. These effective distance contours become closer together in areas of  
135 density vegetation (green) as the resistance parameter  $\alpha_2$  increases. The basis of this as a  
136 model for sound attenuation is clear: individuals vocalizing from a location with high densi-  
137 ties of vegetation (or other structure) between that location and the sensor should produce  
138 reduced signal strength and lowered detection probability due to sound deflection, absorp-



139 tion and other mechanisms. In what follows I describe the model formally and demonstrate  
140 that the actual parameters governing attenuation of the sound can be explicitly estimated  
141 from experimental data on such an array.

142 In practice, this model could be applied in situations where relatively fine scale habitat  
143 structure data are available. For example, in a study of birds on a landscape it might be  
144 possible to obtain such data from auxiliary surveys of vegetation structure but most likely  
145 fine-scale remotely sensed data from aerial imagery, lidar or similar platforms would be  
146 ideal for this purpose. In aquatic environments attenuation is most affected by depth and  
147 sub-surface structure and in most studies of aquatic systems detailed data exist for these  
148 attributes (and others).

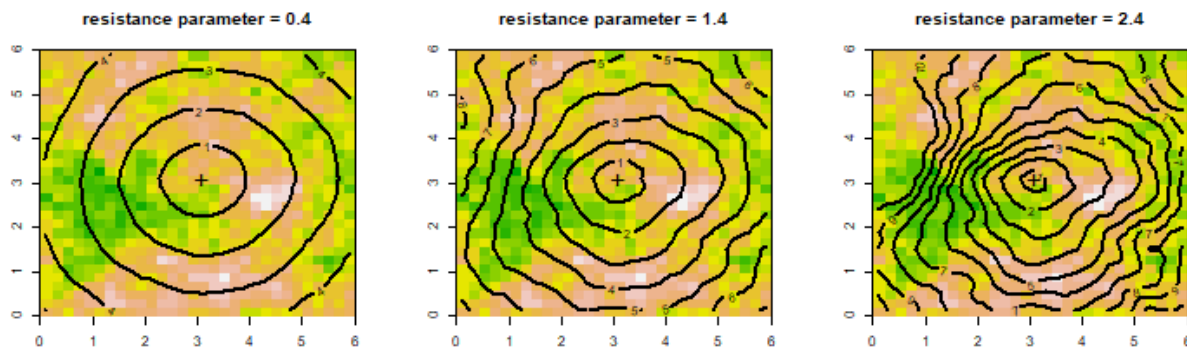


Figure 2: Effective distance to a sensor (shown by +) placed at (3,3) under the least-cost path model with parameter  $\alpha_2 = 0.4$  (left),  $\alpha_2 = 1.4$  (center) and  $\alpha_2 = 2.4$  (right). As resistance increases, effective distance contours get closer together in response to dense structure (green).

### 149 **3 Likelihood Analysis**

The cost-weighted distance metric described above is amenable to direct likelihood analysis from data on observed signal strength at fixed locations and with fixed sources (e.g., as in Fig. 1). The observed data from an experiment are the detection/signal strength pairs  $(y_{ij}, S_{ij})$  for each source and each sensor. Recall that signal strength is truncated at some

value  $c$  chosen to reflect a reasonable threshold below which signals cannot be distinguished from ambient noise. Conditional on the  $J$  known source locations  $\mathbf{x}_j$ , the likelihood for the data from source location  $\mathbf{s}_i$  is

$$\mathcal{L}(\alpha_0, \alpha_1, \alpha_2, \sigma) = \left\{ \prod_{j=1}^J p_{ij}^{y_{ij}} (1 - p_{ij})^{1-y_{ij}} \right\} \left\{ \prod_{y_{ij}=1} f(S_{ij}; \sigma, \alpha_0, \alpha_1, \alpha_2)^{y_{ij}} \right\} \quad (5)$$

150 where  $f(S_{ij}; \sigma, \alpha_0, \alpha_1, \alpha_2)$  is the normal probability density with mean  $\alpha_0 + \alpha_1 d_{cud}(\mathbf{x}_j, \mathbf{s}_i; \alpha_2)$   
151 and variance  $\sigma^2$  and the probability of detection  $p_{ij} = \Pr(S_{ij} > c)$  which depends on the  
152 parameters of the normal distribution model for  $S_{ij}$  in Eq. 4. The likelihood can be optimized  
153 numerically using standard methods such as implemented in the R functions `nlm` or `optim`  
154 (see Appendix A).

### 155 3.1 Unknown source locations

156 The parameters of the attenuation model can be estimated from data obtained when the  
157 sources are unknown. Of course this would be the case in any real field application of bio-  
158 acoustics where animal sounds are measured. Indeed, this is precisely the situation addressed  
159 in spatial capture-recapture applications such as considered by Efford et al. (2009) and  
160 others. In this case, we have to regard the source location as a latent variable and remove  
161 it from the conditional-on-s likelihood (Eq. 5) by integrating over the planar state space  
162 (or 3-dimensional state-space in the context of aquatic systems) in the vicinity of the sensor  
163 array. One twist to the situation where the sources are unknown is the potential exists that  
164 some of the sources were not detected at all. Therefore, the likelihood has to be constructed  
165 either conditional on the event that an individual source was detected at least once (Borchers  
166 and Efford 2008) or else the possibility of  $n_0$  unobserved all-zero encounter histories must  
167 be accounted for, where  $n_0$  is then an additional parameter to be estimated (equivalently  
168  $N = n_0 + n_{obs}$ ). Indeed,  $n_0$  is the key parameter of interest in spatial capture-recapture  
169 applications. See Efford et al. (2009) for details on the likelihood construction. I provide an

170 implementation in R of the likelihood in terms of  $n_0$  in Appendix A.

## 171 3.2 Computing the posterior distribution of a source

Bayes' rule can be used to calculate the posterior distribution of an unobserved source given the pattern of detections,  $\mathbf{y}$ , on the sensor array and the signal strengths,  $\mathbf{S}$ . Note that the likelihood given in Eq. 5 is the joint distribution of the detection/non-detection data  $\mathbf{y}_i$  and the signal strengths  $\mathbf{S}_i$  conditional on the source location  $\mathbf{s}_i$ , say  $\Pr(\mathbf{y}_i, \mathbf{S}_i | \mathbf{s}_i)$ . Let  $\Pr(\mathbf{s})$  denote the prior distribution for  $\mathbf{s}$ , then the posterior distribution of  $\mathbf{s}_i$  is

$$\Pr(\mathbf{s}_i | \mathbf{y}_i, \mathbf{S}_i) = \frac{\Pr(\mathbf{y}_i, \mathbf{S}_i | \mathbf{s}_i) \Pr(\mathbf{s}_i)}{\int_{\mathbf{s}} \Pr(\mathbf{y}_i, \mathbf{S}_i | \mathbf{s}) \Pr(\mathbf{s}) d\mathbf{s}}$$

These probability distributions depend on the model parameters as in the likelihood given above but I omit that dependence to be concise. A standard assumption in spatial capture-recapture is to assume no *a priori* information about the location of a source so that  $\Pr(\mathbf{s}) = \text{constant}$  (Efford et al. 2009) in which case the posterior distribution is just standardized by the integral of the likelihood over the region in the vicinity of the sensor array. More generally, source density gradients can be accommodated by modeling explicit covariate effects in  $\Pr(\mathbf{s})$ . For example, suppose the sound sources are birds and they are likely to be using habitat preferentially, even the same habitat which is affecting sound attenuation, then we might assume

$$\Pr(\mathbf{v}) \propto \exp(\theta z(\mathbf{v}))$$

172 where  $z(\mathbf{v})$  is the measured habitat structure for any location  $\mathbf{v}$  and  $\theta$  is a parameter to be  
173 estimated.

174 R code for computing the posterior distribution of detected sources is given in Appendix  
175 A and I show an example in the following section.

### 176 **3.3 Data acquisition**

177 The model as specified here assumes that unique vocalizations can be identified and recon-  
178 ciled among the detectors. For example this is easily true in an experimental setting when  
179 a sound is played, in which case the sensors at which it is detected can be noted directly.  
180 Over a period of time, each individual source can be played sequentially or even replicated  
181 multiple times. In field settings when the source location is unknown then a specific source  
182 encounter history has to be reconciled in a sense manually. But in practice can be done  
183 unambiguously in many practical settings if the density of sources is not too high (Dawson  
184 and Efford 2009). In the field (sampling real birds), an individual might make many calls  
185 during a particular time interval and these are treated as distinct sources.

## 186 **4 Illustration**

Using the experimental sensor array shown in Fig. 1 I simulated some data under the model for log-signal strength with  $\alpha_0 = 0$ ,  $\alpha_1 = 1.0$  and  $\sigma = 0.50$ . Therefore,

$$S = 0 - 1 \times d_{ij} + \text{normal}(0, \sigma = 0.50).$$

187 I used a threshold of detection of  $c = -3$ . Moreover, the least-cost path distance model of  
188 attenuation was used with  $\alpha_2 = 2.0$  to model attenuation through the heterogeneous habitat  
189 shown in Fig. 1. These parameter settings produce an average of 20.8 total captures of 13.8  
190 individuals on the array of 9 sensors. A particular realization is shown in Fig. 3 which shows  
191 the pattern of detections of the 16 sources. In particular, lines are connected between each  
192 source and the sensor(s) at which it was detected. Three of the sources were not detected at  
193 all, 6 were detected once, 6 were detected twice, and one source three times. The MLEs for  
194 the model parameters for this single realization are  $\hat{\alpha}_0 = -0.155$ ,  $\hat{\alpha}_1 = 0.699$ ,  $\hat{\alpha}_2 = 2.676$  and  
195  $\hat{\sigma} = 0.417$ . In general, a very high level of precision is possible for this relatively low level

196 of detections in an experimental setting when the source locations are known. For example,  
197 100 realizations of this situation produce an MLE of  $\alpha_2$  having mean 1.96 (recall truth =  
198 2.0) and standard error 0.398. The R script for simulating data and fitting the model is  
199 given in Appendix A.

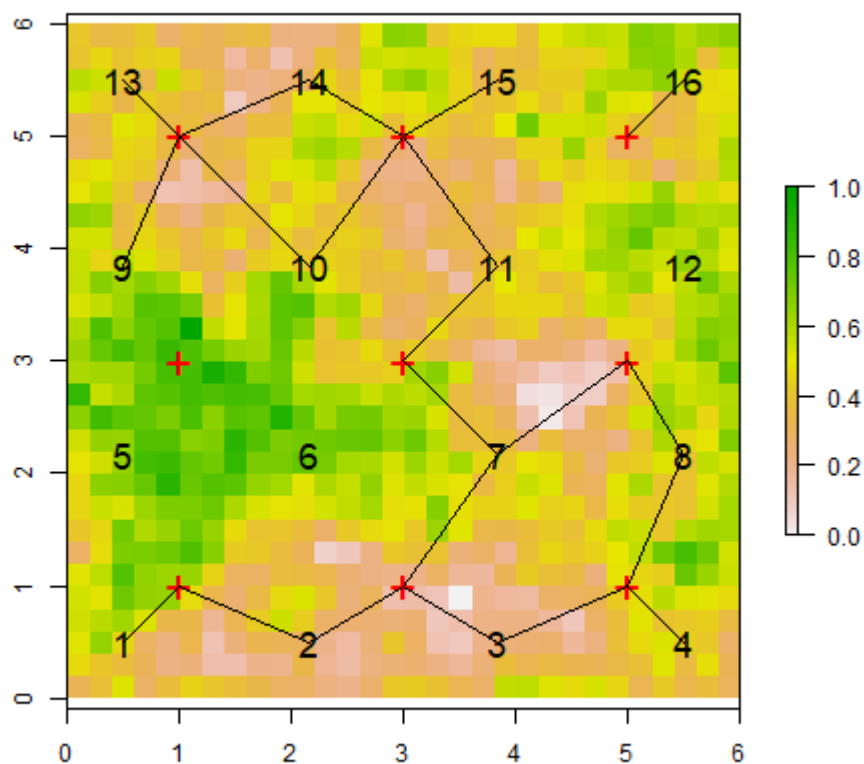


Figure 3: A single realization of a bioacoustic experiment to measure non-Euclidean attenuation in the form of the least-cost path model. For this simulated realization, detection frequencies of the 16 sources as follows: (1, 2, 2, 1, 0, 0, 3, 2, 1, 2, 2, 0, 1, 2, 1, 1). Each source is connected to the sensors at which it was detected.

200 Maximum likelihood estimation for this experimental system is much less effective when  
201 the source locations  $\mathbf{s}$  are *unknown*, in which case the MLEs can be considerably biased (see  
202 Appendix A). Instead, a much larger array is required, or a denser population of sources  
203 is needed in order to generate sufficient encounters. This is consistent with what is known

204 in spatial capture-recapture studies; see for example Efford and Fewster (2013), Sun et al.  
205 (2014) and chapter 10 in Royle et al. (2014)). Nevertheless, it is possible to localize the  
206 unknown sources using the general likelihood formulation based on the marginal likelihood.  
207 For the same simulated data set shown in Fig. 3 I produced the estimated posterior distri-  
208 bution of the unknown source location of 4 sources (Fig. 4) captured between 1 and 3 times  
209 each. We see that the estimated posterior distributions are in the vicinity of the true source  
210 locations, modified by the observed encounter history (the data set is generated using the  
211 random number seed noted in Appendix A).

## 212 5 Discussion

213 With the rapid and expanding adoption of acoustic monitoring technology, the ability to  
214 understand sound attenuation along environmental gradients will become increasingly im-  
215 portant (Kessel et al. 2013). In this paper I suggested a flexible framework for modeling  
216 sound attenuation in heterogeneous environments. This framework has two direct appli-  
217 cations. First, it can lead to improved inferences about source locations (“localization”)  
218 which is important in many applications, especially acoustic telemetry. Second, it allows  
219 investigators to better understand how bioacoustic methods work under field conditions in  
220 heterogeneous environments by enabling *in situ* inference about factors that influence atten-  
221 uation from field data. The method is sufficiently flexible that it can be used with acoustic  
222 telemetry data, as well as encounter history data used in acoustic SCR applications (Efford  
223 et al. 2009; Stevenson et al. 2015; Kidney et al. 2016). I formulated the model here in  
224 terms of “signal strength” data (e.g., sound intensity measured in decibels) but the idea  
225 applies directly when time of arrival data are available. For such data, the localization  
226 model also involves a distance function (Stevenson et al. 2015) which might be replaced by  
227 cost-weighted or least-cost path distance with parameters to be estimated. In addition, the  
228 basic ideas apply directly to classical distance sampling methods (Buckland et al. 2001),

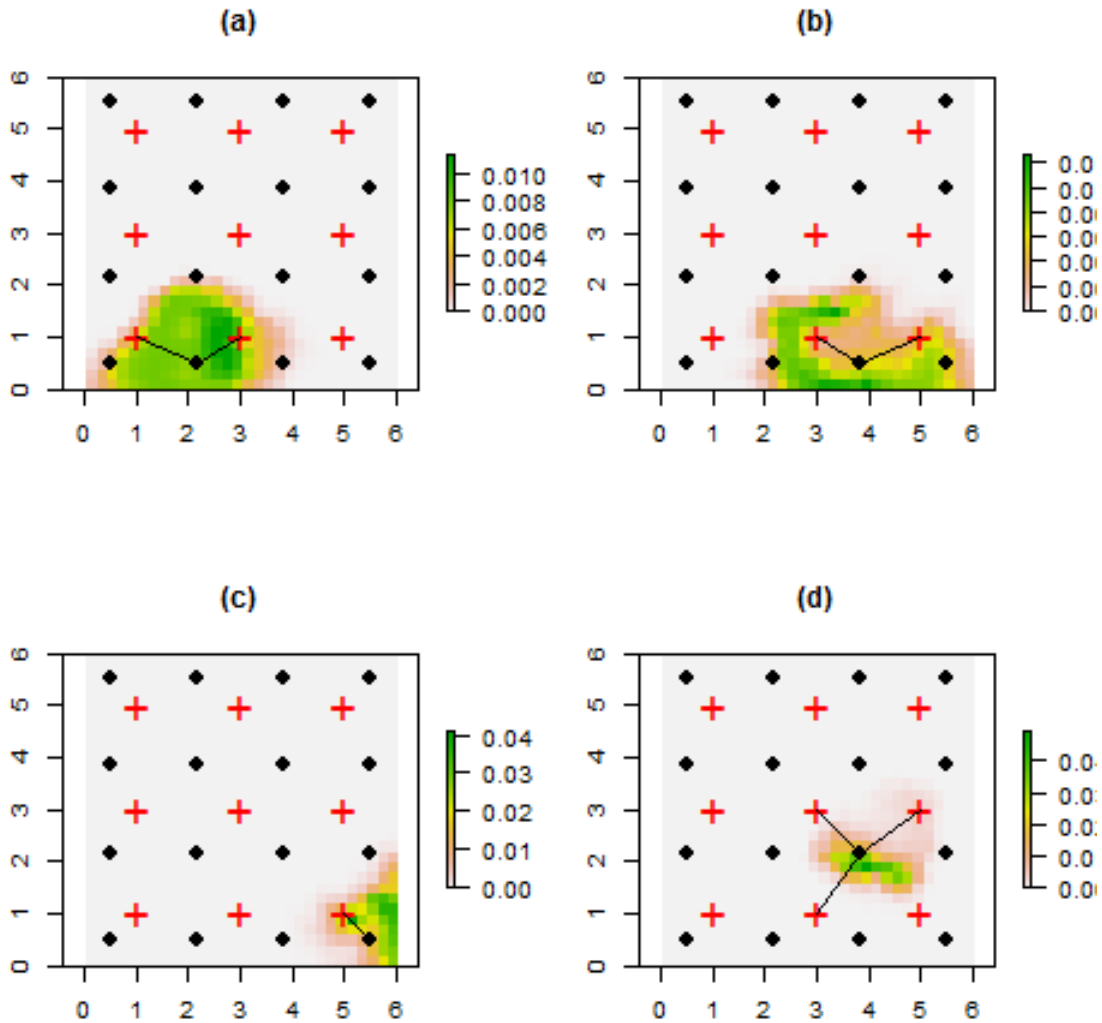


Figure 4: Estimated localizations of 4 unknown sources characterized by the estimated posterior distribution of the source location obtained by plugging-in the MLEs obtained by maximizing the likelihood for the observed detection/non-detection and signal strength data. Because these are posterior distributions the sum over all pixels equals 1.0. For each of the 4 sources shown here the true location of the source is connected to the sensors at which it was detected by lines.

229 where the Euclidean distance metric in the distance sampling likelihood can be replaced by  
230 cost-weighted distance. In the case of distance sampling, in most applications, the model  
231 would provide a description of visual obstruction and not wave attenuation.

232 The ability to develop explicit models of sound attenuation has important sampling de-  
233 sign implications. In heterogeneous environments, the detection range of sensors depends on  
234 environmental characteristics (Kessel et al. 2013; Selby et al. 2016) and thus this critical  
235 parameter is both nonstationary and anisotropic. Therefore, the optimal spacing of sensors  
236 in an array must be variable in response to the underlying environmental heterogeneity. The  
237 problem of array design is analogous to the design of camera trap studies (e.g., Royle et  
238 al. 2014; ch. 10), where arrays can be constructed so as to maximize the probability of  
239 detection, optimize criteria based on the variance of estimators of parameters of interest,  
240 or maximize the precision of the localization. Using the non-Euclidean model of effective  
241 distance suggested in this paper, one could obtain estimates of the parameter  $\alpha_2$  from an  
242 experimental or observational study and then use that estimate to improve the design of bio-  
243 acoustic monitoring arrays. In practice, having multiple sensors in a given experimental array,  
244 with known source locations, such as shown in Fig. 1, is not necessary. One could obtain  
245 suitable estimates of model parameters with a single sensor and replicated source emissions.  
246 However, in field applications of localization or density estimation (such as Dawson and  
247 Efford 2009) multiple sensors are required. In general, estimation of model parameters is  
248 challenging when source locations are unknown and effective estimation might require a a  
249 large array of sensors and a large sample size of detections. As such, in practice, one might  
250 first consider experimental analysis of sound attenuation models with known sources in order  
251 to obtain precise estimates of parameters of the effective distance model which may then be  
252 treated as fixed in subsequent analyses focused on localization or density estimation.

253 An obvious extension of the framework proposed here is to consider alternative non-  
254 Euclidean distance metrics. For example, one obvious alternative is to substitute resistance  
255 distance (McRae 1996) in place of cost weighted distance. Resistance distance is based on



256 an analogy between discrete landscapes (characterized by a raster of pixels) and electrical  
257 circuits. Resistance distance between two nodes is the effective resistance between them,  
258 which depends on the resistance between each node and the number of pathways in the  
259 circuit. I think both cost weighted distance (or least-cost path) and resistance distance offer  
260 useful descriptions of sound attenuation in heterogeneous landscapes.

261 One limitation of the proposed approach is that the cost-weighted distance model under-  
262 lying least-cost path is a phenomenological model. It describes the phenomenon of attenua-  
263 tion in response to measurable covariates but does not explicitly embody elements of sound  
264 dynamics such as reverberation, absorption and reflection. Rather, it models their total ef-  
265 fect as measured by the apparent relative distance between points as measured by observed  
266 signal strength and pattern of detections. This may not be a severe limitation in biological  
267 applications of acoustic monitoring where interest is usually in the end use of the data for  
268 detection, localization or similar objectives and not directly in the processes contributing to  
269 sound dynamics of a particular system.

270 Application of any non-Euclidean effective distance model depends on the availability of  
271 environmental or habitat information at a suitable scale to be relevant to sound dynamics.  
272 While small scale habitat data are not always collected in field studies using acoustic sampling  
273 or distance sampling, it seems likely that such data will be collected more frequently in the  
274 future with the increasing availability of lidar technology (Zolkos et al. 2013, He et al. 2015)  
275 and other remote sensing platforms such as drones (Martin et al. 2012, Christie et al. 2016).

## 276 **Acknowledgments**

277 The author thanks Cathleen Balantic, Danielle Rappaport, Andrew MacLaren and Suresh  
278 Sethi for helpful comments and suggestions on this manuscript. Any use of trade, product,  
279 or firm names is for descriptive purposes only and does not imply endorsement by the U.S.  
280 Government.

## 281 Literature Cited

- 282 Adriaensen, F., J.P. Chardon, G. De Blust, E. Swinnen, S. Villalba, H. Gulinck, and E.  
283 Matthysen. 2003. The application of least-costmodelling as a functional landscape model.  
284 *Landscape and Urban Planning* 64:233-247.
- 285 Blumstein, D.T., D.J. Mennill, P. Clemins, L. Girod, K. Yao, G. Patricelli, et al. 2011.  
286 Acoustic monitoring in terrestrial environments using microphone arrays: applications,  
287 technological considerations and prospectus. *Journal of Applied Ecology* 48:758767.
- 288 Borchers, D.L., and M.G. Efford. 2008. Spatially explicit maximum likelihood methods for  
289 capture-recapture studies. *Biometrics* 64:377-385.
- 290 Borchers, D.L., B.C. Stevenson, D. Kidney, L. Thomas, and T.A. Marques. 2015. A unifying  
291 model for capturerecapture and distance sampling surveys of wildlife populations. *Journal*  
292 *of the American Statistical Association* 110:195-204.
- 293 Bower, J.L., and C.W. Clark. 2005. A field test of the accuracy of a passive acoustic location  
294 system. *Bioacoustics* 15:1-14.
- 295 Brauer, C.L., T.M. Donovan, R.M. Mickey, J. Katz, and B.R. Mitchell. 2016. A comparison  
296 of acoustic monitoring methods for common anurans of the northeastern United States.  
297 *Wildlife Society Bulletin* 40:140-149.
- 298 Buckland, S.T., D.R. Anderson, K.P. Burnham, J.L. Laake, D.L. Borchers, and L. Thomas.  
299 2001. Introduction to distance sampling estimating abundance of biological populations.
- 300 Christie, K.S., S.L. Gilbert, C.L. Brown, M. Hatfield, and L. Hanson. 2016. Unmanned  
301 aircraft systems in wildlife research: current and future applications of a transformative  
302 technology. *Frontiers in Ecology and the Environment* 14:241-251.
- 303 Cooke, S.J., E.G. Martins, D.P. Struthers, L.F. Gutowsky, M. Power, S.E. Doka, J.M.  
304 Dettmers, D.A. Crook, M.C. Lucas, C.M. Holbrook, and C.C. Krueger. 2016. A mov-

305 ing targetincorporating knowledge of the spatial ecology of fish into the assessment and  
306 management of freshwater fish populations. *Environmental monitoring and assessment*  
307 2016:188-239.

308 Crossin, G.T., M.R. Heupel, C.M. Holbrook, N.E. Hussey, S.K. LowerreBarbieri, V.M.  
309 Nguyen, G.D. Raby, and S.J. Cooke. 2017. Acoustic telemetry and fisheries manage-  
310 ment. *Ecological Applications* **27**:1031-1049.

311 Dawson, D.K., and M.G. Efford. 2009. Bird population density estimated from acoustic  
312 signals. *Journal of Applied Ecology* **46**:1201-1209.

313 Digby, A., M. Towsey, B.D. Bell, and P.D. Teal. 2013. A practical comparison of manual  
314 and autonomous methods for acoustic monitoring. *Methods in Ecology and Evolution*  
315 **4**:675-683.

316 Efford, M. G., D.K. Dawson, and D.L. Borchers. 2009. Population density estimated from  
317 locations of individuals on a passive detector array. *Ecology* **90**:2676-2682.

318 Efford M.G., and R.M. Fewster. 2013. Estimating population size by spatially explicit  
319 capture-recapture. *Oikos* **122**:918-28.

320 Fuller, A.K., C.S. Sutherland, J.A. Royle, and M.P. Hare. 2015. Estimating population  
321 density and connectivity of American mink using spatial capture-recapture. *Ecological*  
322 *Applications* **26**:1125-1135.

323 Graves, T.A., R.B. Chandler, J.A. Royle, P. Beier, and K.C. Kendall. 2014. Estimating  
324 landscape resistance to dispersal. *Landscape Ecology* **29**:1201-1211.

325 He, K.S., B.A. Bradley, A.F. Cord, D. Rocchini, M.-N. Tuanmu, S.Schmidtlein, W. Turner,  
326 M. Wegmann, N. Pettorelli. 2015. Will remote sensing shape the next generation of  
327 species distribution models? *Remote Sens Ecol Conserv* **1**:418.

328 Heupel, M.R., J.M. Semmens, and A.J. Hobday. 2006. Automated acoustic tracking of

- 329 aquatic animals: scales, design and deployment of listening station arrays. *Marine and*  
330 *Freshwater Research* **57**:1-13.
- 331 Janik, V.M., S.M. Parijs, and P.M. Thompson. 2000. A two-dimensional acoustic localiza-  
332 tion system for marine mammals. *Marine Mammal Science* **16**:437-447.
- 333 Kessel, S.T., S.J. Cooke, M.R. Heupel, N.E. Hussey, C.A. Simpfendorfer, S. Vagle, and A.T.  
334 Fisk. 2014. A review of detection range testing in aquatic passive acoustic telemetry  
335 studies. *Reviews in Fish Biology and Fisheries* **24**:199-218.
- 336 Kidney, D., B.M. Rawson, D.L. Borchers, B.C. Stevenson, T.A. Marques, and L. Thomas.  
337 2016. An efficient acoustic density estimation method with human detectors applied to  
338 gibbons in Cambodia. *PLOS ONE* **11**:p.e0155066.
- 339 Marques, T.A., L. Thomas, J. Ward, N. DiMarzio, and P.L. Tyack. 2009. Estim-  
340 ating cetacean population density using fixed passive acoustic sensors: an example with  
341 Blainvilles beaked whales. *Journal of the Acoustic Society of America* **125**:1982-1994.
- 342 Marques, T.A., L. Thomas, S.W. Martin, D.K. Mellinger, J.A. Ward, D.J. Moretti, D. Harris  
343 and P.L. Tyack. 2013. Estimating animal population density using passive acoustics.  
344 *Biological Reviews* **88**:287-309.
- 345 Martin, J., H.H. Edwards, M.A. Burgess, H.F. Percival, D.E. Fagan, B.E. Gardner, J.G.  
346 Ortega-Ortiz, P.G. Ifju, B.S. Evers, and T.J. Rambo. 2012. Estimating distribution of  
347 hidden objects with drones: From tennis balls to manatees. *PLoS One* **7**, p.e38882.
- 348 McGregor, P.K., T. Dabelsteen, C.W. Clark, J.L. Bower, and J. Holland. 1997. Accuracy  
349 of a passive acoustic location system: empirical studies in terrestrial habitats. *Ethology*  
350 *Ecology & Evolution* **9**:269-286.
- 351 McRae, B.H. 2006. Isolation by resistance. *Evolution* **60**:1551-1561.
- 352 Measey, G.J., B.C. Stevenson, T. Scott, R. Altwegg, and D.L. Borchers. 2017. Counting

- 353 chirps: acoustic monitoring of cryptic frogs. *Journal of Applied Ecology* 54:894-902.
- 354 Rek, P. and K. Kwiatkowska. 2016. Habitat complexity and the structure of vocalizations: a  
355 test of the acoustic adaptation hypothesis in three rail species (Rallidae). *Ibis* 158:416-427.
- 356 Royle, J.A., R.B. Chandler, R. Sollmann, and B. Gardner. 2014. Spatial Capture-Recapture.  
357 AcademicPress/Elsevier. 612 pages.
- 358 Royle, J.A., R.B. Chandler, K.D. Gazenski, and T.A. Graves. 2013. Spatial capture-  
359 recapture models for jointly estimating population density and landscape connectivity.  
360 *Ecology* 94:287-294.
- 361 Selby, T.H., K.M. Hart, I. Fujisaki, B.J. Smith, C.J. Pollock, Z. HillisStarr, I. Lundgren,  
362 and M.K. Oli. 2016. Can you hear me now? Rangetesting a submerged passive acoustic  
363 receiver array in a Caribbean coral reef habitat. *Ecology and Evolution* 6:4823-4835.
- 364 Singh, L., N.J. Downey, M.J. Roberts, D.M. Webber, M.J. Smale, M.A. Van den Berg,  
365 R.T. Harding, D.C. Engelbrecht, and B.M. Blows. 2009. Design and calibration of an  
366 acoustic telemetry system subject to upwelling events. *African Journal of Marine Science*  
367 31:355-364.
- 368 Stevenson, B.C., D.L. Borchers, R. Altwegg, R.J. Swift, D.M. Gillespie, and G.J. Measey.  
369 2015. A general framework for animal density estimation from acoustic detections across  
370 a fixed microphone array. *Methods in Ecology and Evolution* 6:38-48.
- 371 Sun, C.C., A.K. Fuller, and J.A. Royle. 2014. Trap configuration and spacing influences  
372 parameter estimates in spatial capture-recapture models. *PLOS ONE* 9, e88025.
- 373 Sutherland, C., A.K. Fuller, and J.A. Royle. 2015. Modelling non-Euclidean movement and  
374 landscape connectivity in highly structured ecological networks. *Methods in Ecology and*  
375 *Evolution* 6:69-177.
- 376 van Etten, J. 2017. R Package gdistance: Distances and Routes on Geographical Grids.

377 *Journal of Statistical Software* **76**:1-21.

378 Zolkos, S.G., S.J. Goetz, and R. Dubayah. 2013. A meta-analysis of terrestrial aboveground  
379 biomass estimation using lidar remote sensing. *Remote Sensing of Environment* **128**:289-  
380 298.

381 Wiley, R.H. and D.G. Richards. 1982. Adaptations for acoustic communication in birds:  
382 sound transmission and signal detection. *Acoustic Communication in Birds* **1**:131-181.

## 383 Appendix A

```
384 # This block of code simulates a habitat landscape in the vicinity of a sensor array
385
386 B = 3
387 lambda = B/3 # correlation range for habitat map
388 library(raster)
389 library(scrbook)
390 set.seed(1234)
391 # raster grid
392 delta <- (2 * B - 0)/30
393 grx <- seq(delta/2, 2 * B - delta/2, delta)
394 gr <- expand.grid(grx, grx, KEEP.OUT.ATTRS = FALSE)
395
396 V <- exp(-e2dist(gr, gr)/lambda)
397 x <- t(chol(V)) %*% rnorm(900)
398
399 # png("system.png")
400 op <- par(mar = c(3, 3, 3, 6))
401 on.exit(par(op))
402 habrast<-rasterFromXYZ(cbind(as.matrix(gr), x))
403 # Standardize the covariate to be in [0,1]
404 vv<- values(habrastr)
405 vv<- vv-min(vv)
406 vv<- vv/max(vv)
407 values(habrastr) <- vv
408 image(habrastr, col=rev(terrain.colors(20)), asp = 1, bty = "n")
409
410 rect(0, 0, 2 * B, 2 * B)
411 # Define array of sensors
```

```
412 sensors<- as.matrix(expand.grid(seq(1,5,2),seq(1,5,2)))
413 points(sensors, pch = "+", cex = 3)
414 image.scale(vv, col=rev(terrain.colors(20)) )
415
416 # Define some sources (speakers playing recorded calls)
417 X<- as.matrix(expand.grid(seq(0.5, 5.5,,4), seq(0.5, 5.5,,4) ) )
418 points(X,pch=3, cex=3,col="red", lwd=3)
419 # dev.off()
420
421
422 # Define some parameter values for the signal strength model. Supposes a suitable
423 # transformation of signal strength is normal
424 alpha0<- -2
425 # thinking about alpha1 being related to the range parameter of a half-normal in order to
426 alpha1<- -(1/(2*1*1))
427 D<- e2dist(X, sensors)
428 S<- matrix(NA,nrow=nrow(D),ncol=ncol(D))
429 for(i in 1:nrow(S)){
430   S[i,]<- rnorm(ncol(D),alpha0 + alpha1*D, 0.5) # sigma = 0.5 here
431 }
432 # Detection occurs if signal strength > - 3 . Threshold is arbitrary, more or less.
433 y<- (S> -3)
434 y
435 sum(y)
436
437 vv<- values(habrast)
438 vv<- vv-min(vv)
439 vv<- vv/max(vv)
440 values(habrast)<- vv
441 plot(habrast)
442 image(habrast, col=rev(terrain.colors(20)))
443 image.scale(values(habrast), col=rev(terrain.colors(20)))
444 title("Vegetation density")
445 points(3.1,3.1, pch = "+", cex = 2)
446 gr<-coordinates(habrast) #####
447
448 #
449 # Next block of code computes the effective distance matrix for some value
450 # of alpha2 which is specified in the for loop initiation. This is done
451 # so that the Figure in the manuscript can be produced if a vector of
452 # values is specified
453 #
454 library(gdistance)
```

```
455 #png("3rasters.png",width=720,height=240)
456 par(mfrow=c(1,3) )
457 # pick values of alpha2 here to evaluate the effective distance. I'm using 2 but the
458 # figure from the manuscript uses c(0.4, 1.4, 2.4)
459 for(alpha2 in c( 2) ){
460 cost<- exp( alpha2*habrast ) # lots of attenuation through dense cover
461 tr1<-transition(cost,transitionFunction=function(x) 1/mean(x),directions=16)
462 tr1CorrC <-geoCorrection(tr1,type="c",multpl=FALSE,scl=FALSE)
463 dcost <-costDistance(tr1CorrC, X, sensors)
464 dcost.rast<- costDistance(tr1CorrC, as.matrix(gr), sensors)
465 # could use accCost for EACH sensor location and then pull out the
466 # values needed.... This is a bit tedious so just use least-cost path.
467 # r1<- accCost(tr1CorrC, sensors[1,])
468 # incell<- rep(NA,nrow(sensors))
469 # for(j in 1:nrow(sensors)){
470 # dd<- e2dist(sensors,coordinates(r1))
471 # dd2<- apply(dd,1,min)
472 # incell[j]<- (1:ncol(dd))[dd[j,]==dd2[j]]
473 #}
474 r<- cost
475 values(r)<- dcost.rast[,5] # column 5 corresponds to the center sensor
476 image(habrast, col=rev(terrain.colors(20)),xlab=" ",ylab=" ")
477 title(paste("resistance parameter = ",theta,sep=""),cex=6)
478
479 points(3.1,3.1, pch = "+", cex = 2)
480 contour(r, levels= c(1, 2, 3, 4, 5, 6, 7, 8, 9, 10), add=TRUE, lwd=2)
481 }
482
483 #dev.off()
484
485 # Example of simulating the attenuated signal
486 D<- dcost
487 # D<- e2dist(X,sensors) # Could use Euclidean distance here
488 alpha0<- -0.5
489 alpha1<- 1
490 Sh<- matrix(NA,nrow=nrow(D),ncol=ncol(D))
491 for(i in 1:nrow(Sh)){
492   Sh[i,]<- rnorm(ncol(D),alpha0 - alpha1*D[i,], 0.5)
493 }
494 cut<- -3
495 y<- (Sh> cut)
496 Sh[y==0]<-NA
497
```



```
498 apply(y,1,sum)
499 y<- as.numeric(y)
500
501
502 # This is the likelihood for fixed sources, uses fixed distance matrix
503 # not estimated
504 lik<-function(parms, D){
505 alpha0<- parms[1]
506 alpha1<- (parms[2])
507 sigma<- exp(parms[3])
508
509 ES<- alpha0 - alpha1*D
510 gamma <- ( cut - ES )/sigma
511
512 phi <- pnorm(gamma, 0, 1)
513 p <- 1-phi
514 dn <- dnorm(Sh, ES, sigma)
515
516 ll1<- -1*sum(log(apply((p^y)*(1-p)^(1-y),1,prod))) -1*( sum(log(dn[y==1])) )
517 ll1
518 }
519 # obtain the MLEs
520 tmp<-nlm(lik,c(alpha0, alpha1, -1),D=dcost, hessian=TRUE)
521 c(tmp$estimate[1], (tmp$estimate[2]),exp(tmp$estimate[3]))
522
523
524
525 # This function computes the likelihood for fixed sources assuming the
526 # resistance parameter is a parameter to be estimated...
527
528 likknownS<-function(parms,yamat){
529 alpha0<- parms[1]
530 alpha1<- parms[2]
531 alpha2<- parms[3]
532 sigma<- exp(parms[4])
533
534 cost<- exp( alpha2*habrast ) # lots of attenuation through dense cover
535 tr1<-transition(cost,transitionFunction=function(x) 1/mean(x),directions=16)
536 tr1CorrC <-geoCorrection(tr1,type="c",multpl=FALSE,scl=FALSE)
537 dcost <-costDistance(tr1CorrC, X, sensors)
538
539 D<- dcost
540 ES<- alpha0 - alpha1*D
```

```
541 gamma <- ( cut - ES )/sigma
542
543 phi <- pnorm(gamma, 0, 1)
544 p <- 1-phi
545 dn <- dnorm(Sh, ES, sigma)
546 ll1<- -1*sum(log(apply((p^ymat)*((1-p)^(1-ymat)),1,prod))) -1*( sum(log(dn[ymat==1])) )
547 return(ll1)
548 }
549
550
551 # Simulation code. Change "nsims" to do more than 1.
552
553 simout<- NULL
554 nsims<- 1
555 set.seed(123)
556
557 for(sim in 1:nsims){
558
559 # Simulate a data set using the cost distance specified above
560 D<- dcost
561 alpha0<- 0
562 alpha1<- 1
563 nreps<- 3 # In an experimental setting we would do multiple replicates from each sensor
564 cut<- -3
565 ymat<- Sh<- array(NA,dim=c(nreps, nrow(D),ncol(D)))
566 for(r in 1:nreps){
567 for(i in 1:nrow(D)){
568 Sh[r,i,]<- rnorm(ncol(D),alpha0 - alpha1*D[i,], 0.5)
569 ymat[r,i,]<- as.numeric(Sh[r,i,]>cut)
570 }
571 }
572 # Just keep 1 rep for the illustration. Likelihood is not set up for replicates
573 Sh<- Sh[1,,]
574 ymat<- ymat[1,,]
575
576 # Plot the detection data from 1 realization of the experimental setting
577 #png("1realization.png",width=480,height=480)
578 do<- 1:nrow(ymat)
579 prast<- habrast
580 plot(prast)
581 points(sensors, pch = "+", cex = 2,col="red")
582 points(X, pch= " ")
583 text(X, as.character(do),cex=1.5)
```

```
584 for(i in do){
585   a<- ymat[i,]
586   if(sum(a)==0) next
587   b<- matrix(sensors[a==1,],ncol=2,byrow=FALSE)
588   for(j in 1:nrow(b)){
589     lines(rbind(X[i,],b[j,]))
590   }
591 }
592 #dev.off()
593
594
595 # Obtain the MLE of the known-s model
596
597 tmp<-nlm(likknownS,c(0,1,2,0),hessian=TRUE,ymat=ymat)
598 parms1<- c(tmp$estimate[1],tmp$estimate[2],tmp$estimate[3],exp(tmp$estimate[4]))
599 names(parms1)<- c("alpha0","alpha1","alpha2","sigma")
600 (parms1)
601
602 # Fit the model with s not known
603
604 # First discard the all-zero data from the sources that were not detected
605 ncap<- apply(ymat,1,sum)
606 rownames(ymat)<- 1:nrow(ymat)
607 ymat<- ymat[ncap>0,]
608 Sh<- Sh[ncap>0,]
609 Sh[ymat==0]<- NA
610 gr<-coordinates(habrast)
611 gr<- as.matrix(gr)
612
613 # Should be defined outside of the simulation loop
614 lik<-function(parms,ymat, gr, compute.post=FALSE){
615   alpha0<- parms[1]
616   alpha1<- parms[2]
617   alpha2<- parms[3]
618   sigma<- exp(parms[4])
619   N<- nrow(ymat) + exp(parms[5])
620
621   cost<- exp( alpha2*habrast ) # lots of attenuation through dense cover
622   tr1<-transition(cost,transitionFunction=function(x) 1/mean(x),directions=16)
623   tr1CorrC <-geoCorrection(tr1,type="c",multpl=FALSE,scl=FALSE)
624   dcost <-costDistance(tr1CorrC, gr, sensors)
625
626   ymat<- rbind(ymat, rep(0,ncol(ymat)))
```

```
627 post<- matrix(NA,nrow=nrow(ymat),ncol=nrow(gr))
628 Sh<- rbind(Sh, rep(NA,ncol(ymat)))
629 nind<- nrow(ymat)-1
630 D<- dcost
631 ES<- alpha0 - alpha1*D
632 gamma <- ( cut - ES )/sigma
633 phi <- pnorm(gamma, 0, 1)
634 p <- 1-phi
635
636 lik1<- lik2<-rep(NA,nrow(ymat))
637 for(i in 1:nrow(ymat)){
638   lik.gr<- ( ( t(p)^ymat[i,] )*( t(1-p)^(1-ymat[i,]) ) )
639   lik.gr<- apply(lik.gr,2,prod) # joint likelihood for each grid pixel
640   lik1[i]<- mean(lik.gr)
641   log.dn<-dnorm(matrix(Sh[i,],nrow=nrow(gr),ncol=ncol(Sh),byrow=TRUE), ES, sigma,log=TRUE)
642   dn<- exp(rowSums(log.dn, na.rm=TRUE))
643   post[i,]<- lik.gr+dn
644   lik2[i]<- mean(dn)
645 }
646 if(!compute.post){
647   nv<- c( rep(1,nind), N-nind)
648   ll<- -1*(lgamma(N) - lgamma(N-nind) + sum(nv*log(lik1)) + sum(nv*log(lik2)) )
649   return(ll)
650 }
651 if(compute.post){
652   post<-post/rowSums(post)
653   return(post)
654 }
655 }
656 }
657
658 # Fit the unknown sources model
659 gr<- coordinates(habrast)
660 tmp<-nlm(lik,c(0,1,2,-1,-1),hessian=TRUE,ymat=ymat,gr=gr)
661
662 parms2<- c(tmp$estimate[1],tmp$estimate[2],tmp$estimate[3],exp(tmp$estimate[4]),
663 exp(tmp$estimate[5]) )
664 names(parms2)<- c("alpha0","alpha1","alpha2","sigma","n0")
665 parms2
666
667 simout<- rbind(simout, c(nind=sum(ncap>0),totcap=sum(ncap),parms1,parms2))
668 }
669
```

```
670 #
671 # Compute the posterior distribution using the MLEs
672 #
673 gr<- coordinates(habrast)
674 post<-lik(tmp$estimate,ymat=ymat,gr=gr,compute.post=TRUE)
675
676 ##### png("posts.png",width=480,height=480)
677 par(mfrow=c(2,2))
678 do<- 2:5 # I will plot the posterior distribution for sources in rows 2-5 of ymat
679 source.ids<- as.numeric(dimnames(ymat)[[1]][do])
680 #prast<-rasterFromXYZ(cbind(gr,post[2,]))
681 # note: wrong order of coordinates
682 prast<- habrast
683 m<- 1
684 for(i in do){
685 prast<- habrast
686 values(prast)<- post[i,]
687 plot(prast)
688 points(sensors, pch = "+", cex = 2,col="red")
689 points(X,pch=20,cex=2)
690 a<- ymat[i,]
691 if(sum(a)==0) next
692 b<- matrix(sensors[a==1,],ncol=2,byrow=FALSE)
693
694 for(j in 1:nrow(b)){
695 lines(rbind(X[source.ids[m],],b[j,]))
696 }
697
698 title( c("(a)","(b)","(c)","(d)") [m] )
699 m<- m+1
700
701 }
702 ##### dev.off()
703
```